TCAD simulation I

E. Giulio Villani

Overview

- **Introduction, needs for TCAD simulations**
- **Transport regimes and related equations**
- **Discretization techniques: meshing**
- **Discretization of semiconductor equations: Scharfetter-Gummel technique**
- **Examples**

Introduction

- TCAD (Technology Computer Aided Design) divides into three groups:
  - **Process simulation**, i.e. simulation of fabrication process steps (oxidation, implantation, diffusion…)
  - **Device simulation**, i.e. simulation of the thermal/electrical/optical behavior of electronic devices,(IV,CV, frequency response…)
  - **Device modeling**, i.e. creating compact behavioral models for devices for circuit simulation (SPICE, Cadence…)

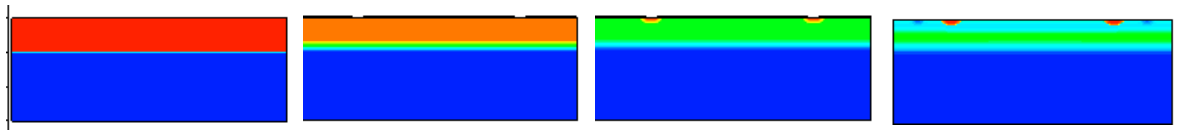

Epitax growth *SiO_2 etch* *N^{++} implant* *P^{++} implant*

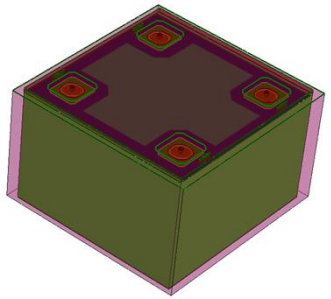

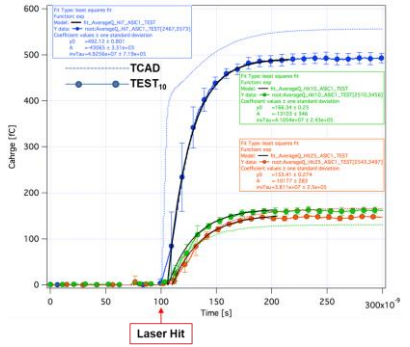

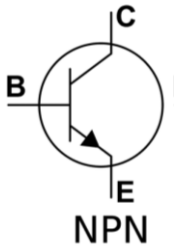

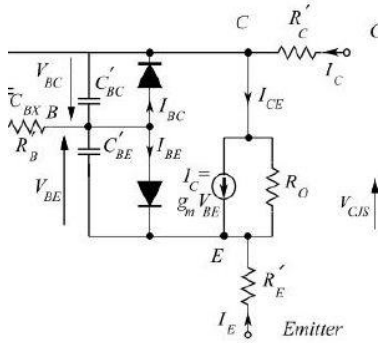

Introduction

- Reasons why TCAD simulations are needed:
  - Market demands cycle of design to production of 18 months or less. Typically 2-3 months required for wafer tape out implies short time for development
  - Reduce cost to run experiments on new devices and circuits

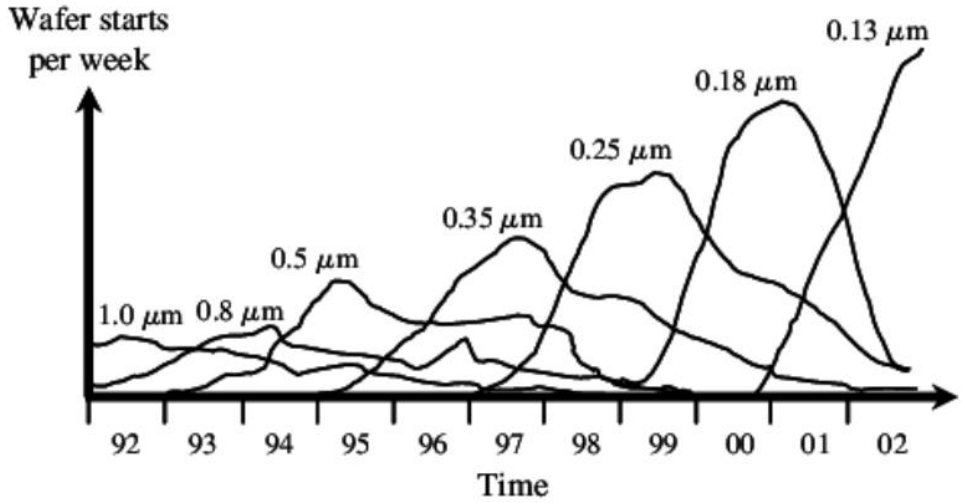

Shrinking product life cycles in semiconductor industry over time

Hochbaum, Dorit S. et al., Rating Customers According to Their Promptness to Adopt New Products., Operations Research, vol. 59, no. 5, p. 1171–83, 2011.

Introduction

- Main components of semiconductor device simulation include fabrication process, description of electronic structure, driving forces and transport phenomena

- The two kernels of semiconductor transport equations and fields that drive charge flow are coupled to each other and needs solving self-consistently

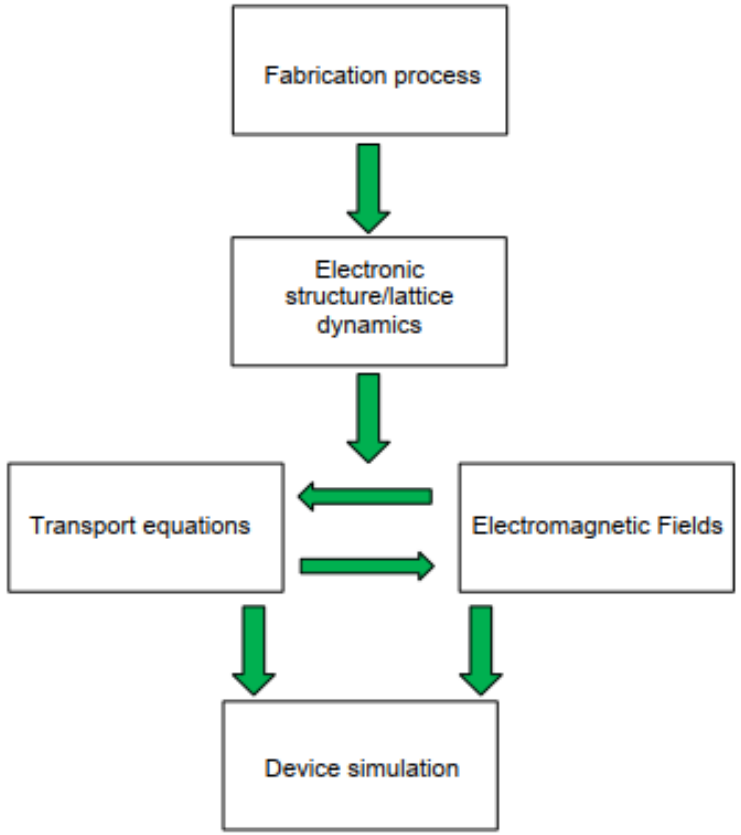

Transport regimes

- Usually only the quasi-static electric fields from the solution of Poisson's equation are necessary
- Transport regime in semiconductors depends on length scale

Modern Silicon technology already requires tools to describe transport in quantum regime [D. K. Ferry and S. M. Goodnick, Transport in Nanostructures, 1997]

	$L \ll l_{e-ph}$			$L \sim l_{e-ph}$	$L \gg l_{e-ph}$
	$L < \lambda$	$L < l_{e-e}$	$L \gg l_{e-e}$		
Transport regime	Quantum	Ballistic	Fluid	Fluid	Diffusive
Scattering	Rare	Rare	*e–e* (Many), *e–ph* (Few)		Many
Model:					
Drift-diffusion					
Hydrodynamic	Quantum hydrodynamic				
Monte Carlo					
Schrödinger equation / Green's function					
Applications	Nanowires, superlattices	Ballistic transistor	Present time ICs	Present time ICs	Older ICs

L: device length
$l_{e\text{-}e}$: electron-electron scattering length
$l_{e\text{-}ph}$: electron-phonon scattering length
λ: electron wavelength

D. Vasileska, et al., Computational Electronics: Semiclassical and Quantum Device Modelling and Simulation, RC press, 2010,ISBN-13: 978-1-4200-6484-1.

Transport regimes

- Charge carrier dynamics in Si detectors usually does not require QM
- Semiclassical laws of motions apply
- Drift-diffusion (DD) equations are often valid, i.e. provided the electron gas is in thermal equilibrium with lattice temperature ($T_e = T_L$)

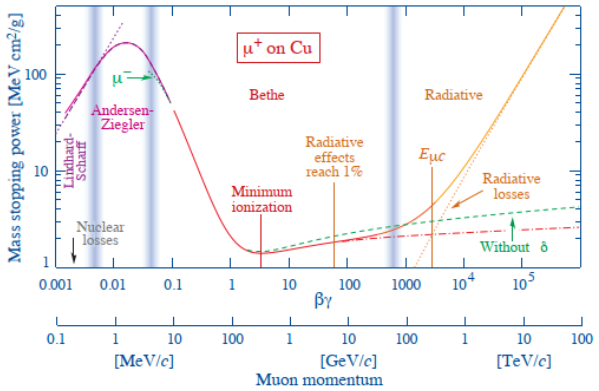

Mass stopping power (= −dE/dx) for positive muons in copper as a function of βγ = p/Mc.

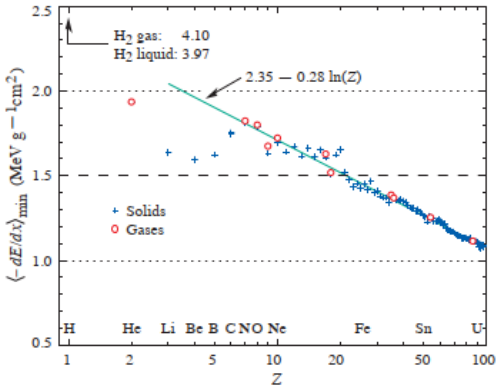

Mass stopping power at minimum ionisation for different chemical elements.

$$R \sim \frac{\hbar}{2\pi}\frac{\gamma v}{<I>} \cong 3.5\ [nm]\ Ionization\ radius\ for\ MIP\ in\ Si^{*}$$

$$n = \frac{dE}{dx}\rho\frac{L}{E_{th}}\frac{1}{\pi R^2 L} \sim 2.5 \cdot 10^{18}\ MIP\ charge\ density\ within\ Ionization\ radius$$

$$\lambda \leq \frac{h}{\sqrt{2meV_b}} \sim \begin{cases} 0.38\ [nm]@10\ V \\ 0.12\ [nm]@100\ V \end{cases} De\ Broglie\ wavelength\ of\ carriers\ @\ full\ depletion$$

[*] E. Segre', Nuclei and Particles, 1st ed. W.A. Benjamin, Inc, New York, 1965.

Drift diffusion model

- The semiconductor equations derived from 0th and 1st moment of BTE are referred to as **Drift-Diffusion*** model
- The model consists of Poisson's equation and PDEs: the continuity and current density equations for electrons and holes
- They express charge and momentum conservation
- Their self-consistent solutions are obtained via discretisation, using finite element methods (FEM)

$$\boldsymbol{\partial_t f + u \cdot \nabla_r f + \frac{F}{\hbar} \cdot \nabla_k f = \mathbf{C}[\mathbf{f}]} \quad \textbf{BTE}$$

$$\nabla \cdot J_n - q\frac{\partial n}{\partial t} = qR$$

$$\nabla \cdot J_p + q\frac{\partial p}{\partial t} = -qR$$

Continuity equations

$$J_n = qn\mu_n E + qD_n \nabla n$$

$$J_p = qp\mu_p E - qD_p \nabla p$$

Current density equations

$$\nabla \cdot \varepsilon_S \nabla \varphi = e(n - p - N_D + N_A)$$

Poisson's equation

*W. Van Roosbroeck, *Theory of flow of electrons and holes in germanium and other semiconductors*, Bell System Technical Journal, vol. 29, p. 560-607, 1950.

Discretization and meshing

- The device simulations process consists of two steps:

1. The test volume is obtained through grid generation (‘mesh generation’)

2. Solving the discretized differential equations using Finite-Boxes method (box integration method) . This method integrates the PDEs over a test volume

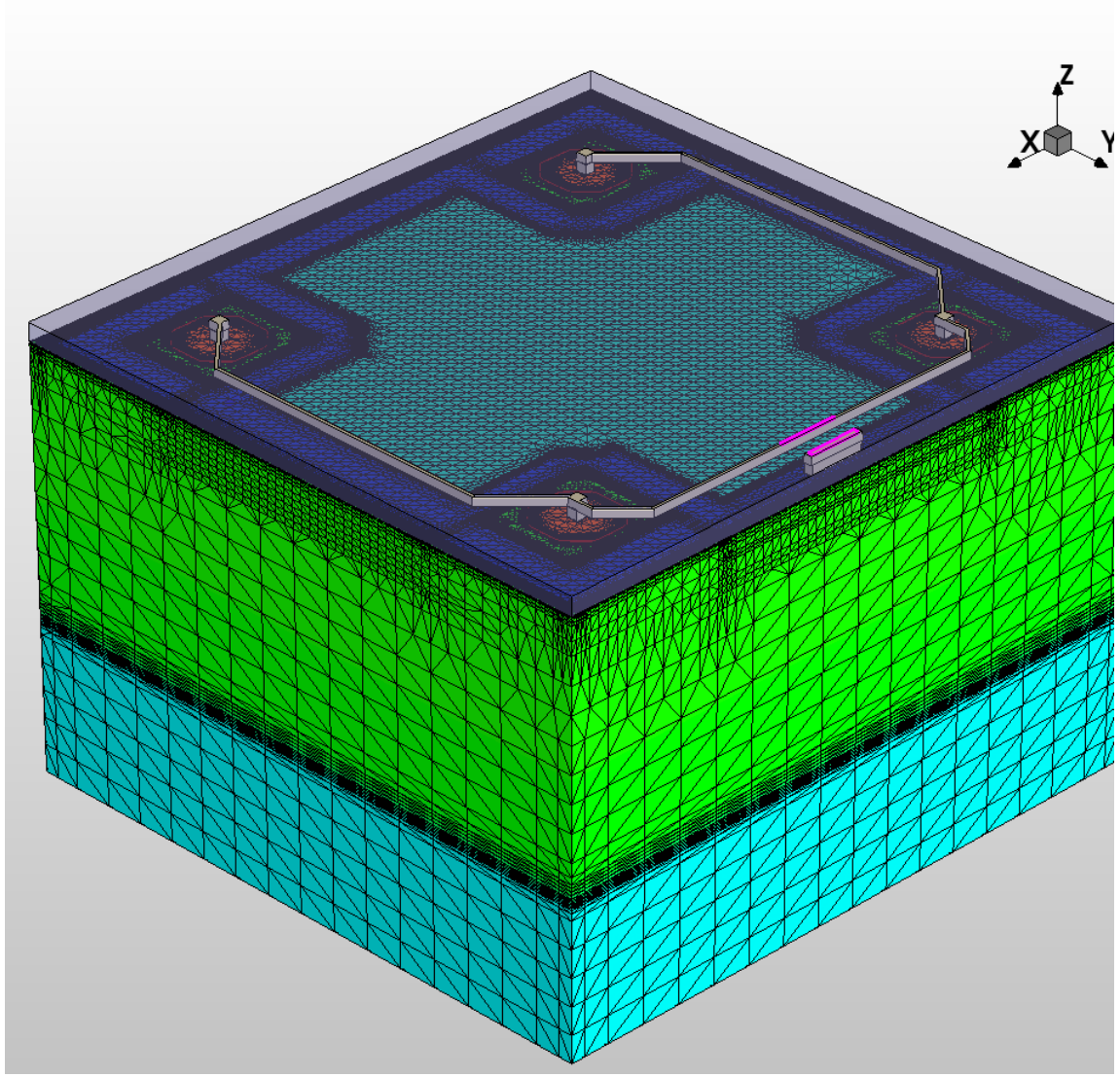

Discretization and meshing

- The meshing used in most FEM methods relies on Delaunay triangulations:

the interior of the circumsphere of each element contains no mesh vertices.

- The Delaunay triangulation of a discrete point set **P** in general corresponds to the dual graph of the Voronoi diagram for **P**

the set of all locations x closest to $P_i \in P$ than to any other point of the grid

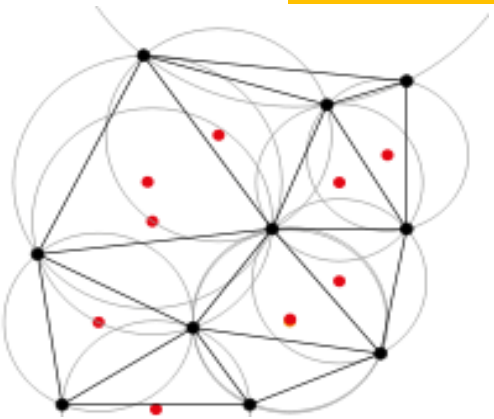

The Delaunay triangulation with all the circumcircles and their centres

$$T_{\mathrm{D},k}(\mathcal{P}_{\mathrm{D},k}) \Longleftrightarrow \exists\, \mathbf{x}$$
$$\mathbf{x} \in \Omega \quad \wedge$$
$$|\mathbf{x}-\mathbf{x}_i| = |\mathbf{x}-\mathbf{x}_j| \;\; \forall \; P_i, P_j \in \mathcal{P}_{\mathrm{D},k} \quad \wedge$$
$$|\mathbf{x}-\mathbf{x}_i| < |\mathbf{x}-\mathbf{x}_k| \;\; \forall \; P_i \in \mathcal{P}_{\mathrm{D},k}, P_j \notin \mathcal{P}_{\mathrm{D},k}$$

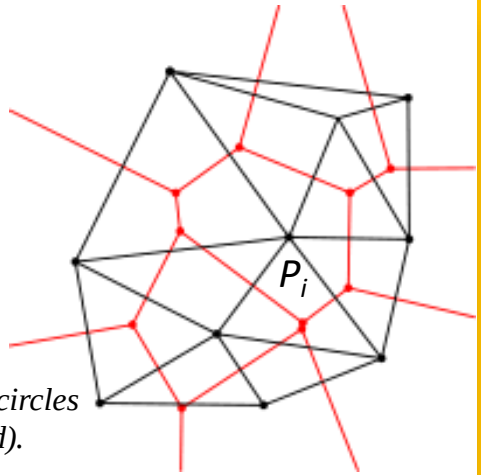

Connecting the centres of the circumcircles produces the Voronoi diagram (in red).

$$\Omega_i = \{\mathbf{x} \;\mid\; |\mathbf{x}-\mathbf{x}_i| \leq |\mathbf{x}-\mathbf{x}_j| \;\; \forall \; i \neq j, \; \mathbf{x} \in \Omega\}$$

Discretization and meshing

- Correct Delaunay triangulation* guarantees element-volume conservation, important in many problems (diffusion, charge generation, et cetera)
- Delaunay triangulation maximises the minimum angle of the triangle

*A. Okabe, B. Boots, and K. Sugihara, ***Spatial Tessellations***, John Wiley and Sons Ltd, 1992.*

Voronoi boxes do not overlap (each circumcircle does not include a point of another triangle). Each can be uniquely assigned to its corresponding grid points.

$$P_i = V_i$$

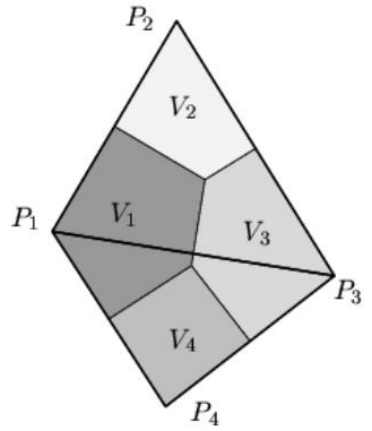

Voronoi boxes do overlap (each circumcircle does include a point of another triangle). Each cannot be uniquely assigned to its corresponding grid points. Wrong volumes calculated

$$P_1 = V_1 + V_5 + V_6$$

$$P_3 = V_3 + V_5 + V_6$$

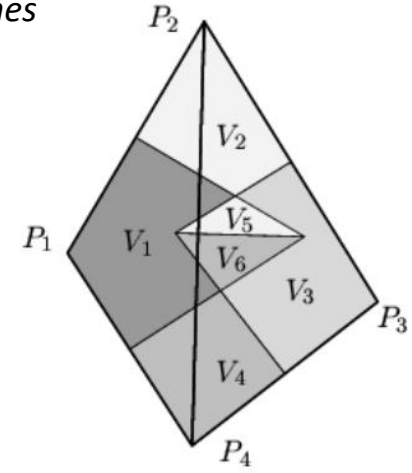

Discretization and meshing

- The discretisation of equations imposes some constraints on spatial and temporal mesh size
- The mesh size should be smaller than the **Debye length** (i.e. the characteristic length for screening of field by charges) where charge variations in space have to be resolved

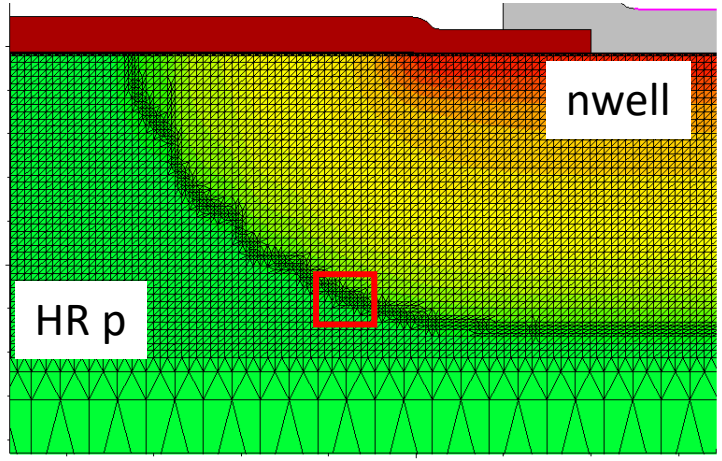

$$L_D = \sqrt{\frac{\varepsilon_s k_B T}{e^2 N}} \; Debye\ length$$

$$N = 10^{13}[cm^{-3}]: L_D \approx 1.3\ [um] @ T = 300\ [K]$$
$$N = 10^{17}[cm^{-3}]: L_D \approx 13\ [nm] @ T = 300\ [K]$$
$$N = 10^{19}[cm^{-3}]: L_D \approx 1.3\ [nm] @ T = 300\ [K]$$

Discretization and meshing

- The temporal ‘mesh’ size should be smaller than the **dielectric relaxation time** t_{dr} (i.e. time it takes to charge fluctuations to decay under the field they produce)
- Time interval smaller than t_{dr} might give unrealistic transient results (‘oscillations’ in estimated transient currents)

$$\tau_{dr} \sim \frac{\varepsilon_s}{eN\mu} \; Dielectric\ relaxation\ time$$

$$N = 10^{13}[cm^{-3}], \mu_n \approx 1400\ \left[[cm^{-3}V^{-1}s^{-1}\right] @ T = 300\ [K]: \tau_{dr} \approx 400\ [ps]$$

$$N = 10^{15}[cm^{-3}], \mu_n \approx 1350\ \left[[cm^{-3}V^{-1}s^{-1}\right] @ T = 300\ [K]: \tau_{dr} \approx 4.8\ [ps]$$

$$\frac{\partial \Delta n}{\partial t} = -\frac{\Delta n(t=0)}{t_{dr}}$$

$$\Delta n\ (\Delta t) = \Delta n\ (0) - \Delta t \frac{\Delta n(0)}{t_{dr}}$$

Box integration method

- The discretisation of Poisson's and continuity equations is done via Box Integration method

- The LHS of equations is transformed via Gauss' theorem and integrated over a Voronoi box Ω_k of point P_k

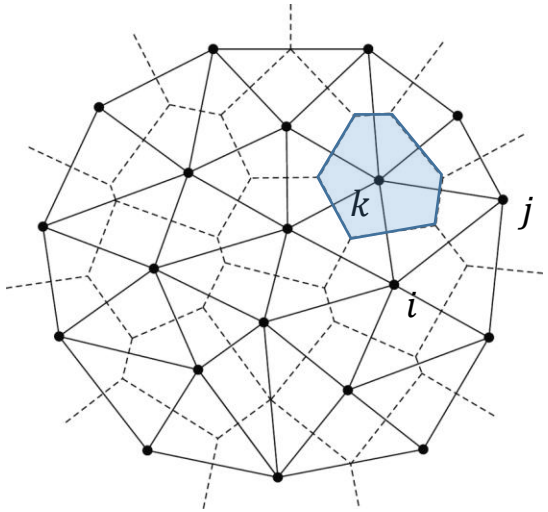

$$\nabla \cdot \varepsilon_S \nabla \varphi = e(n - p - N_D + N_A) \qquad \equiv \int D \cdot dS = \int \rho dV$$

$$\nabla \cdot J_n - q\frac{\partial n}{\partial t} = qR$$

$$\nabla \cdot J_p + q\frac{\partial p}{\partial t} = -qR$$

Box integration method

- Example of **Poisson's equation discretisation**

- Assume that the electric potential is linearly varying over each elementary domain

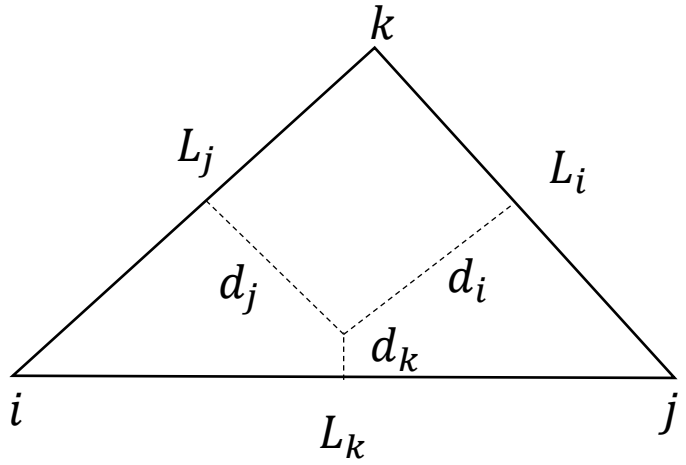

$$\nabla \cdot \varepsilon_S \nabla \varphi = e(n - p - N_D + N_A) \equiv \int D \cdot dS = \int \rho dV$$

i, j, k: *nodal indices*

$\boldsymbol{L_i}, \boldsymbol{L_j}, \boldsymbol{L_k}$: *side vectors*

L_i, L_j, L_k: *magnitude side vectors*

$$u \coloneqq \frac{e}{k_B T} \varphi: \textit{normalized potential}$$

Box integration method

- Components of D vector along sides $L_{i,j,k}$
- Flux of D vector associated to node k:
- The discretisation of RHS is obtained by multiplying the node value of charge by the area of the portion of the Voronoi box

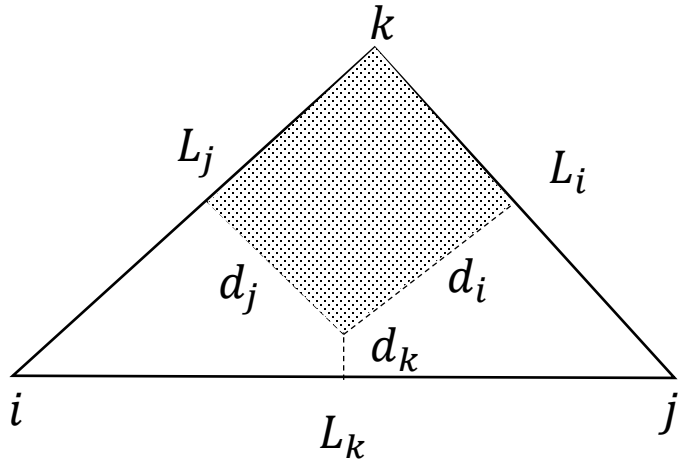

$$\frac{k_B T}{e}\varepsilon_s \frac{1}{L_i}(u_j - u_k)$$
$$\frac{k_B T}{e}\varepsilon_s \frac{1}{L_j}(u_k - u_i)$$
$$\frac{k_B T}{e}\varepsilon_s \frac{1}{L_k}(u_i - u_j)$$

$$\frac{k_B T}{e}\varepsilon_s\left[\frac{d_i}{L_i}(u_j - u_k) + \frac{d_j}{L_j}(u_i - u_k)\right] \quad Flux\ of\ D$$

Box integration method

- Summing over all points P_k of Voronoi boxes

- Same approach to discretise the **continuity equations** for electrons and holes

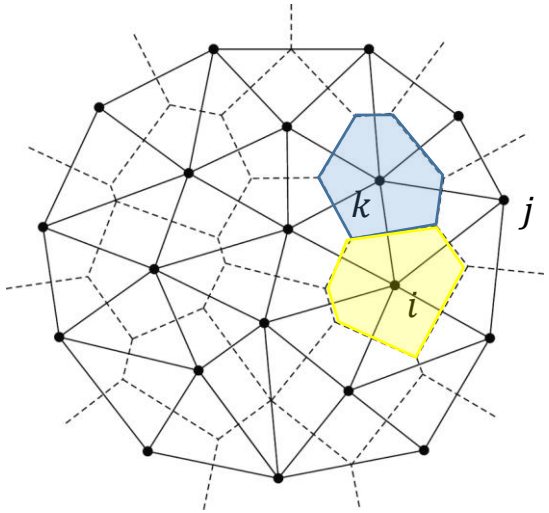

$$\sum_k D_{ik} A_{ik} = \rho_k V_k$$

A_{ik}: *area of* $K - Vbox$
D_{ik}: *projection along grid line*

$$\sum_k J_{n,ik} A_{ik} = q(R_k + \frac{d}{dt} n_k) V_k$$

$$\sum_k J_{p,ik} A_{ik} = -q(R_k + \frac{d}{dt} p_k) V_k$$

Scharfetter-Gummel discretisation

- In case of no strong generation-recombination the current density varies little within each domain
- Even so, this implies an exponential dependence of electron / hole density n/p with position along grid's edge
- Using previous discretization method would require very dense mesh: the Scharfetter-Gummel technique* includes such dependence, requiring less grid points

*D. L. Scharfetter and H. K. Gummel, "Large-signal analysis of a silicon read diode oscillator," IEEE Trans. Electron Devices, vol. ED-16, pp. 64–77, Jan. 1969

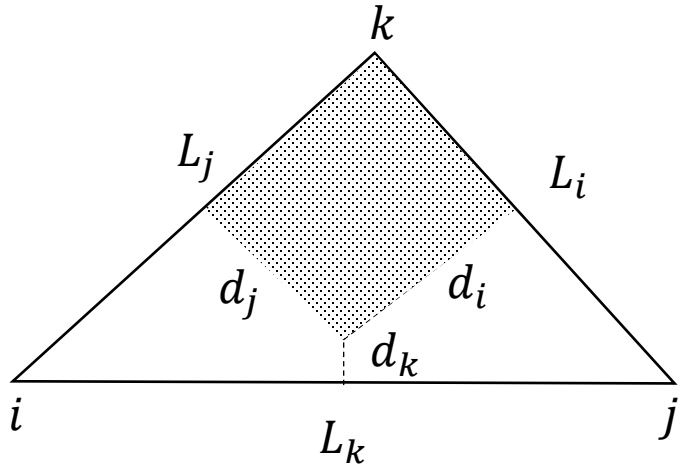

$$J_n = qn\mu_n E + qD_n \nabla n$$

$$J_p = qp\mu_p E - qD_p \nabla p$$

$$u \coloneqq \frac{e}{k_B T}\varphi \qquad D_n \coloneqq \frac{k_B T}{e}\mu_n$$

$$J_n \coloneqq qD_n[\nabla n - n\nabla u] \qquad from\, J_n$$

$$J_{nk} \coloneqq qD_n\left[\frac{dn}{dl_k} - n\frac{du}{dl_k}\right] \qquad projection\ along\ L_k \sim constant$$

Scharfetter-Gummel discretisation

- Assume u varies linearly along the edge and current density $J_n \simeq$ constant over the domain

- Define the reduced current j_{nk} and assume an average diffusion D_{nk} along the edge

- Obtain first order equation in n along the edge

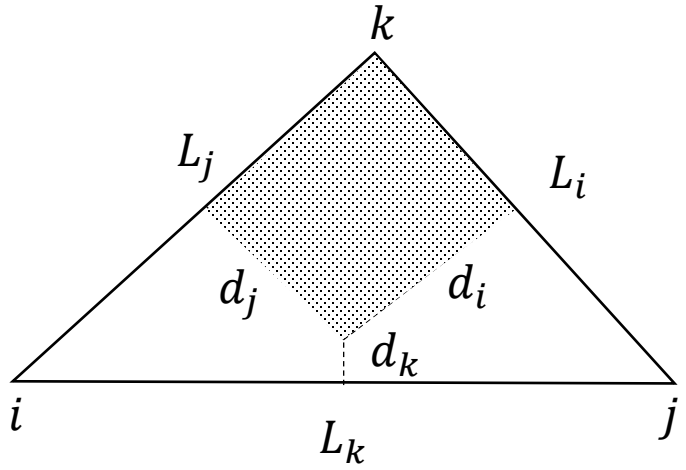

$$u = \frac{u_j - u_i}{L_k} l_k + u_i = a_k l_k + u_i$$

$$j_{nk} := \frac{J_{nk}}{qD_{nk}}, \qquad D_{nk} := < D_{ni}, D_{nj} >$$

$$j_{nk} = \frac{dn}{dl_k} - na_k$$

Scharfetter-Gummel discretisation

- Integrate from node i to node j, i.e. for l_k=[0, L_k]
- Obtain expression relating potential and carriers concentration

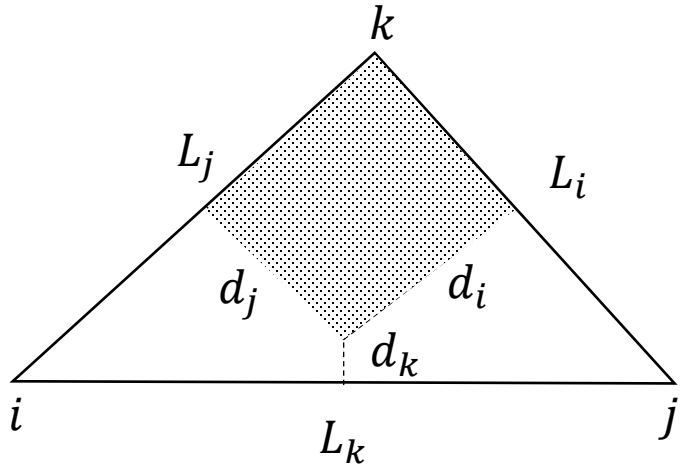

$$\int_0^{L_k} \exp(-a_k l_k)\, j_{nk} = \int_0^{L_k} \exp(-a_k l_k)\left(\frac{dn}{dl_k} - n a_k\right) d\, l_k$$

$$= \int_0^{L_k} \frac{d}{dl_k}(\exp(-a_k l_k) n) dl_k$$

$$j_{nk} \frac{1}{a_k}(1 - \exp(-u_{ji}) = \exp(-u_{ji}) n_j - n_i$$

$$j_{nk} = a_k\left(\frac{n_j}{\exp(u_{ji}) - 1} + \frac{n_i}{\exp(-u_{ji}) - 1}\right)$$

Scharfetter-Gummel discretisation

- Obtain the flux of current density relative to node k

- The Scharfetter –Gummel discretisation requires less fine mesh as the exponential dependence of carriers concentration is included in the discretisation scheme

- It also depends on boundary values, i.e. 2D and 3D cases can be reduced to local 1D cases

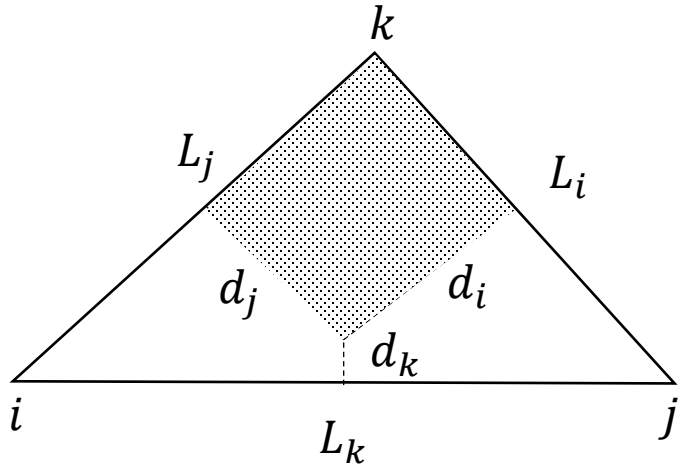

$$j_{nk} = \frac{1}{L_k}\left(\frac{u_{ji}n_j}{\exp(u_{ji})-1} - \frac{u_{ij}n_i}{\exp(u_{ij})-1}\right)$$

$$j_{nk} = \frac{1}{L_k}\left(B(u_{ji})n_j - B(u_{ij})n_i\right) \quad Bernoulli\ function\ B(x) = \frac{x}{\exp(x)-1}$$

$$\nabla \cdot J_{nk}$$
$$= \mathrm{q}D_{ni}\frac{d_i}{L_i}\left(B(u_{jk})n_j - B(u_{kj})n_k\right) + \mathrm{q}D_{ni}\frac{d_j}{L_j}\left(B(u_{ik})n_i - B(u_{ki})n_k\right)$$

Simulation examples

- Examples from Synopsys TCAD (more on this from N. Owen lectures)
- Beside electrical simulation, process simulation is possible
- Most of the typical steps of fabrication process can be simulated

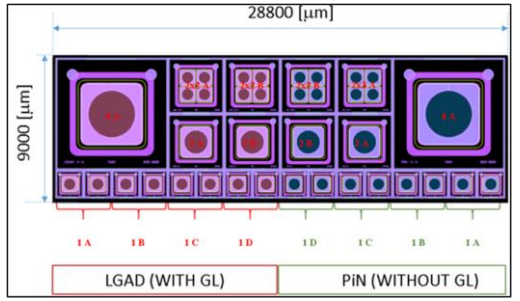

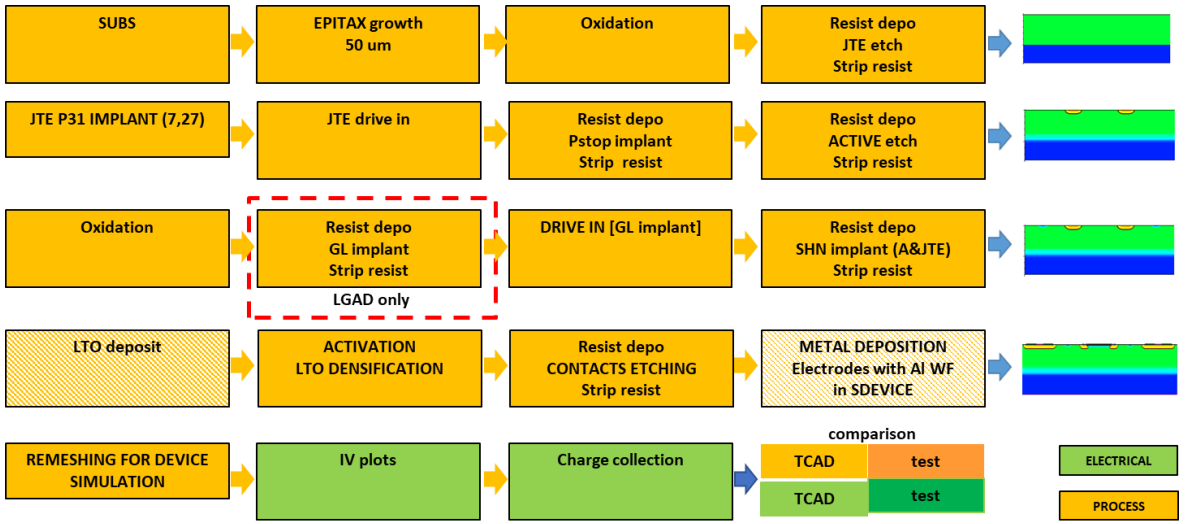

Simulated process steps for LGAD fabrication

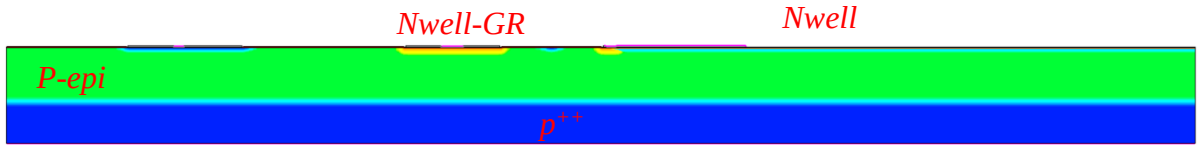

Simulation examples

- Fabrication process and Electrical performances simulation of a Low Gain Avalanche Detector (LGAD*) sensor
- The simulation of the fabrication included photolithography, etching, implantation, diffusion, metal deposition
- The electrical simulations included charge collection and gain due to impact ionisation w.r.t to a PIN diode

*G. Pellegrini, et al., ***Technology developments and first measurements of low gain avalanche detectors (LGAD) for high energy physics applications***, Nuclear Instruments and Methods in Physics Research Section A: Accelerators, Spectrometers, Detectors and Associated Equipment, vol. 765, p. 12 – 16, 2014.*

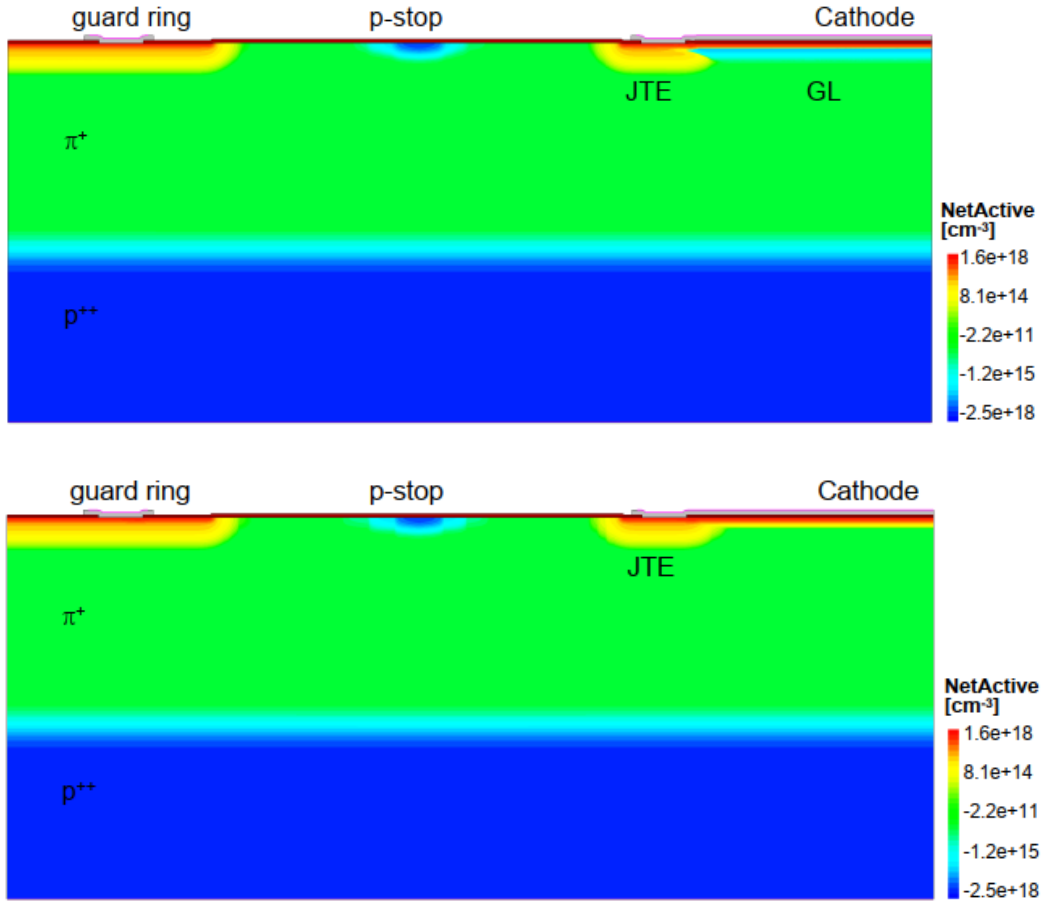

Cross section of simulated LGAD (top) and PIN diode (bottom)

Simulation examples

- High energy implants of ions were simulated, both analytically or through Monte Carlo

- Results compared with Secondary Ion Mass Spectrometry (SIMS): Accuracy ≃ 10% or better

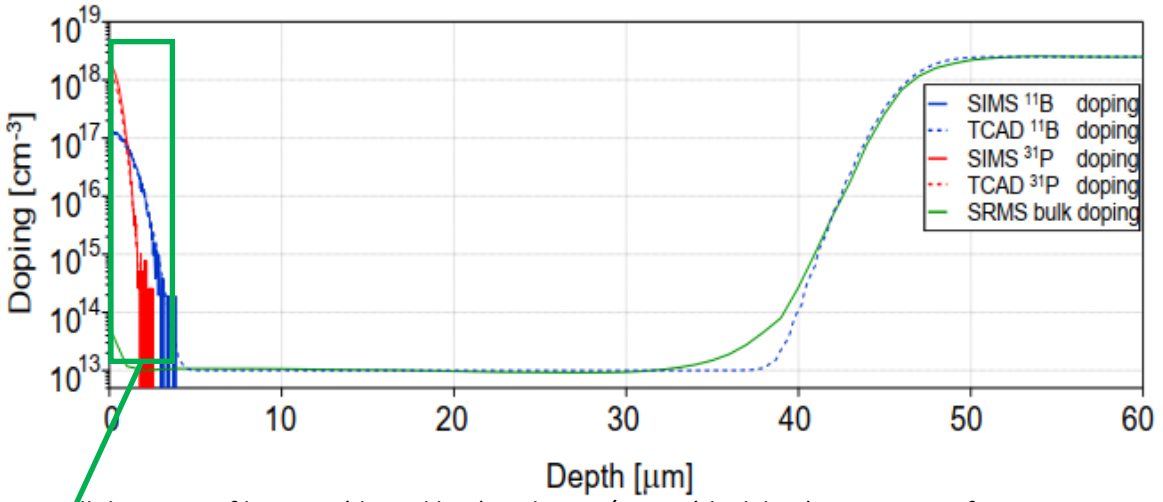

Full doping profile TCAD (dotted line) and SIMS/SRMS (thick line) comparison for LGAD.

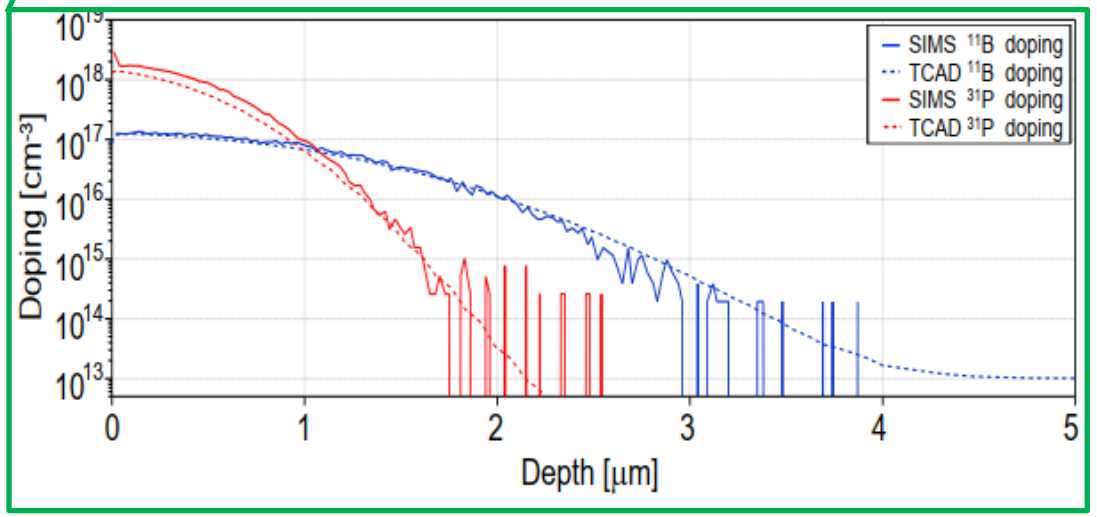

An expanded view of GL doping. SIMS (thick line) and TCAD (dotted line) results are shown for comparison

Simulation examples

- A note on ion implantation:
  - At least with As, MC (SRIM) and SPROCESS predictions on doping seem to agree within ≈ 20%
  - SRIM assumes amorphous Si, <100> used for SPROCESS

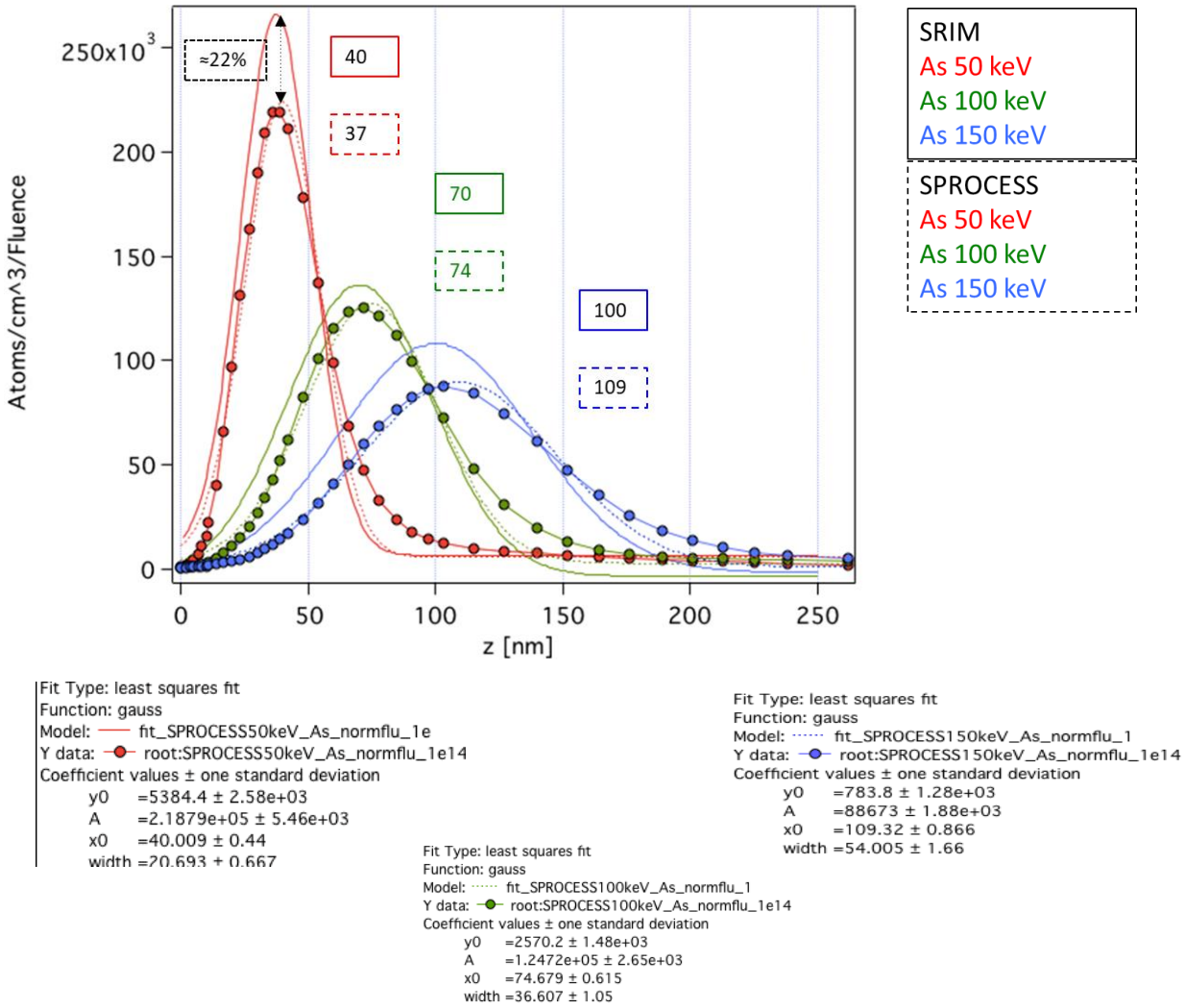

Simulation examples

- Internal field configuration vs. bias and temperature

- DC and AC characteristics can be obtained from the simulated model

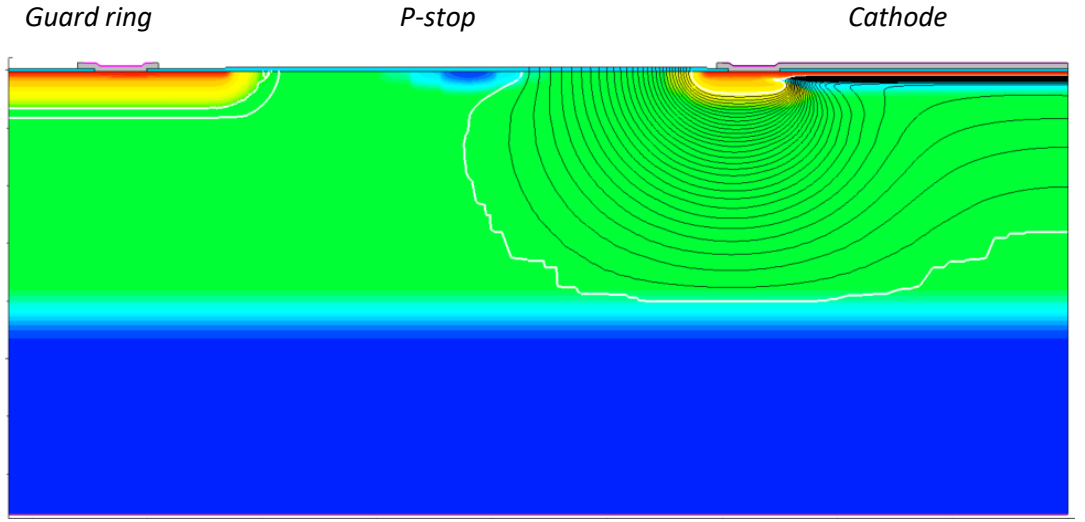

LGAD electrical simulation, showing the extension of depletion region (white line) and equipotential lines (black lines)

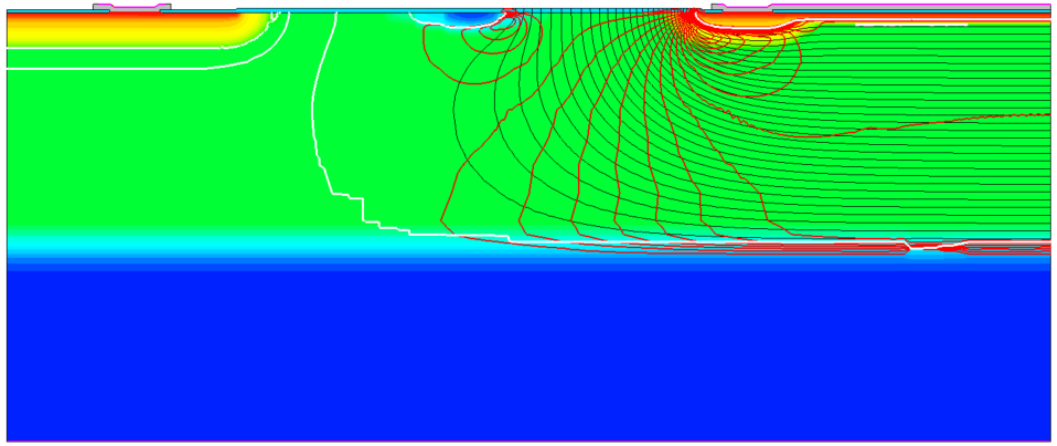

PIN electrical simulation, showing the extension of depletion region (white line), equipotential lines (black lines) and vertical electrical field (red lines)

Simulation examples

- Charge collection is simulated using laser light and MIP injection

- Spatial-temporal meshing different for Light and MIP injection

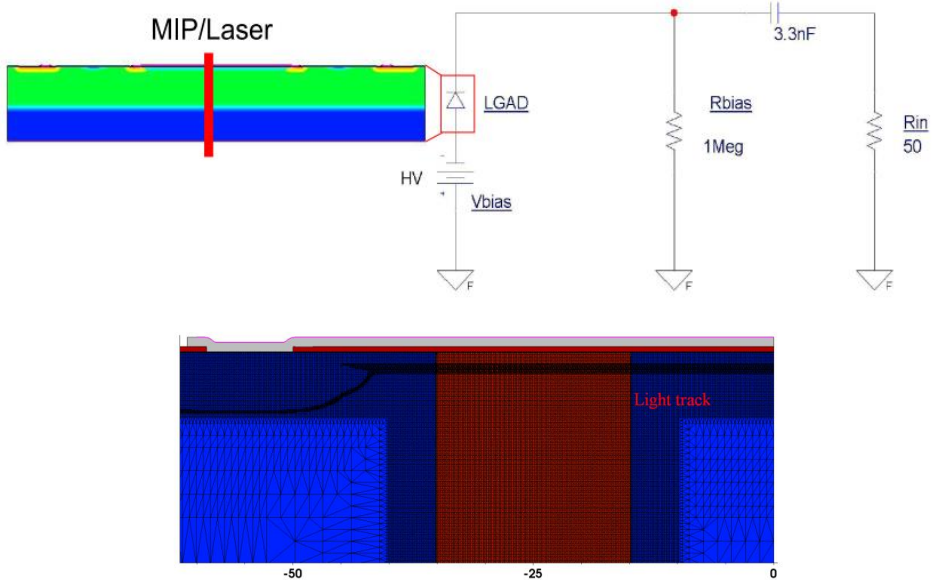

Device meshing for an optical charge injection in the PIN diode. The same meshing resolution was used for LGAD devices. Values in µm.

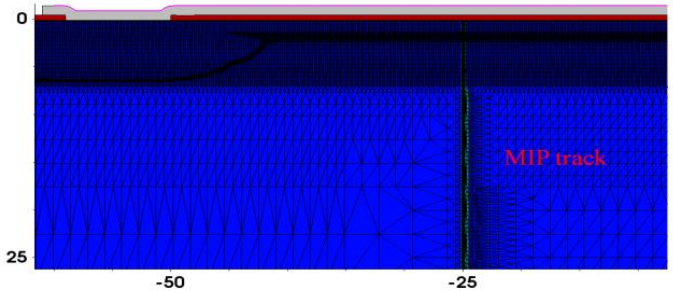

Device meshing for MIP charge injection. A meshing resolution of up to 0.3 nm was used in the radial direction along the MIP track. Values in µm.

Simulation examples

- The gain of the LGAD is defined as the ratio of collected charge w.r.t. the charge collected by a PIN diode, under the same biasing condition
- The gain depends on the bias voltage applied, as this affects the impact ionisation, leading to charge multiplication
- Different impact ionisation models predict different gain

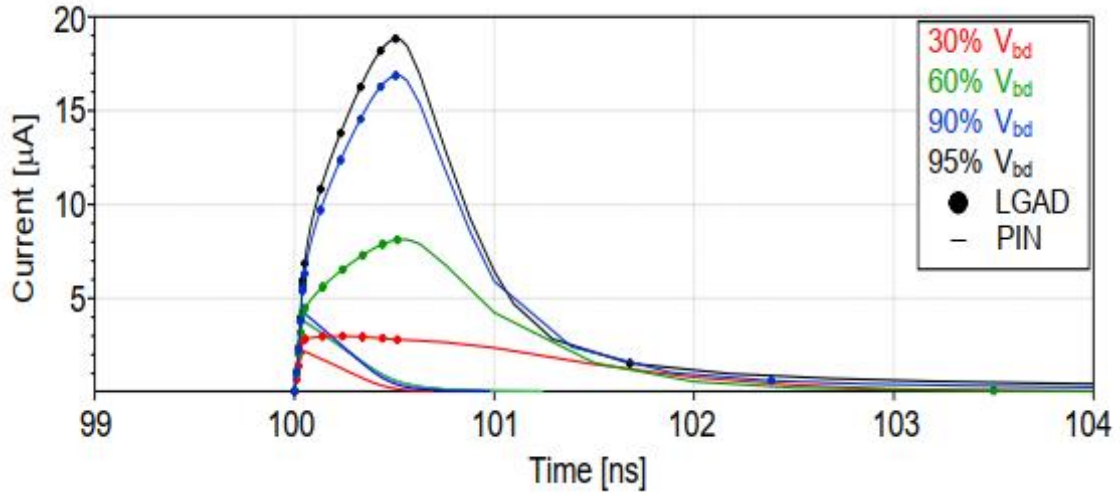

The transient current from optical charge injection in a PIN diode (line) and an LGAD (line with markers) at different percentage of breakdown voltage Vbd. The simulation uses the Okuto impact ionisation model with default values and T = 21 °C.

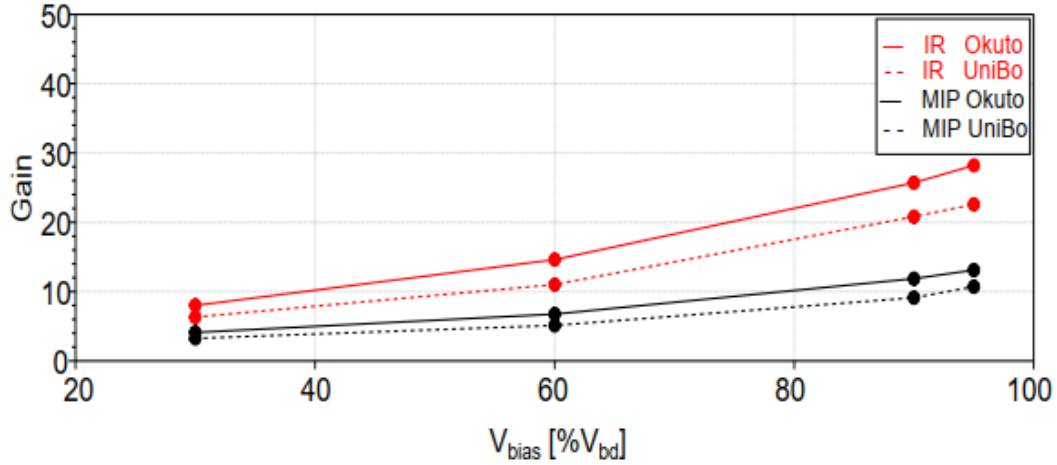

The simulation results of gain normalized to the percentage of V^{bd} using MIP and IR charge injection for an LGAD.

Simulation examples

- The TCAD simulations using the Okuto-Crowell model* for impact ionisation match the measured LGAD gain up to values of the bias voltage of approximately 80% of the breakdown.

- Additional corrections to the modelling are needed to improve the accuracy of prediction

- Due to the exponential dependence of impact ionisation on field / doping / parameters the task of LGAD modelling presents interesting challenges

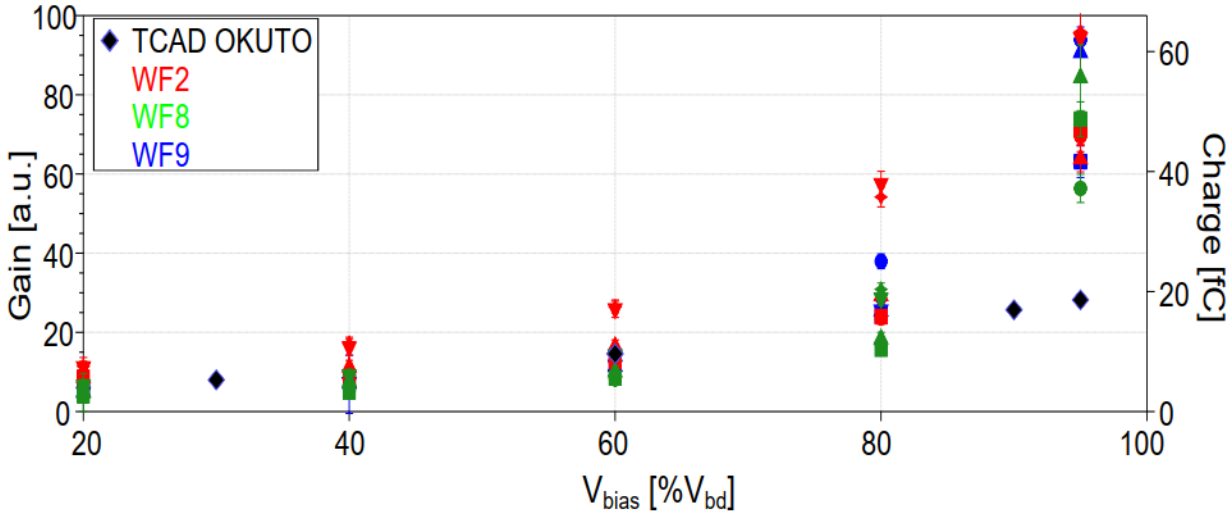

Laser gain and charge collected of five LGAD devices vs. bias normalized to breakdown. The TCAD gain obtained from a laser injection, when the bias voltage is normalized to the breakdown voltage, matches the results up to approximately 80% of the breakdown.

**Y. Okuto and C. R. Crowell, Threshold Energy Effect on Avalanche Breakdown Voltage in Semiconductor Junctions, Solid-State Electronics, vol. 18, no. 2, p. 161–168, 1975.*

Thank you

giulio.villani@stfc.ac.uk

- Introduction to simulation
- Needs and transport regimes
- Meshing and discretization. Intro to DD model discretization. SG method
- Some examples of TCAD simulations: process and electrical device simulations, charge collection